

**Petrogenetic linkages among martian basalts. Implications based on trace element chemistry of olivine.** C.K. Shearer<sup>1</sup>, P.V. Burger<sup>1</sup>, J.J. Papike<sup>1</sup>, L.E. Borg<sup>2</sup>, A.J. Irving<sup>3</sup>, and C.D.K. Herd<sup>4</sup>, <sup>1</sup>Institute of Meteoritics, Department of Earth and Planetary Sciences, University of New Mexico, Albuquerque, New Mexico 87131 ([cshearer@unm.edu](mailto:cshearer@unm.edu)), <sup>2</sup>Lawrence Livermore National Laboratory, Livermore, CA 94551. <sup>3</sup>Department of Earth and Space Sciences, University of Washington, Seattle, WA 98195, <sup>4</sup>Department of Earth and Atmospheric Sciences, University of Alberta, Edmonton, Alberta, Canada T6G 2E3.

**Introduction** Herd et al. [1], Herd [2], Wadhwa [3] and Goodrich et al. [4] demonstrated that the  $f_{O_2}$  in martian basalts represented by the shergottites varies by 2 to 4 log units and is correlated with geochemical parameters such as LREE/HREE, initial  $^{87}\text{Sr}/^{86}\text{Sr}$ , and initial  $\epsilon_{\text{Nd}}$ . These correlations have been interpreted as indicating the presence of reduced, incompatible element-depleted and oxidized, incompatible element-enriched reservoirs that were produced during early stages of martian differentiation ( $\approx 4.5\text{Ga}$ ) [1,2,3,4,5,6,7]. Martian basaltic magmatism represented by the shergottites is thought to represent mixing between these two reservoirs. Whether this mixing process is a product of assimilation or mixing of two mantle reservoirs during melting is still a point of debate.

Perhaps, further insights into the petrogenesis of the shergottites may be acquired through the major and trace element study of one of the earliest phases (olivine) in some of the more primitive shergottites (olivine-phyric shergottites) [4]. Numerous papers have suggested a wide range of petrogenetic relationships between the large olivine crystals found in shergottites and the basaltic melt. The suggested petrogenesis of olivine in the olivine-phyric basalts include phenocrystic olivine, minor accumulation of phenocrystic olivine, accumulation of megacrysts of olivine from the same overall system, and xenocrystic olivine that was randomly incorporated into the basalt. Here, we define the petrogenesis of olivine in the olivine-phyric shergottites, evaluate its use in recording the earliest stages of martian basalt crystallization, and compare olivine in olivine-phyric shergottites to olivine in other martian basaltic lithologies (nahklites, lherzolitic shergottites).

**Analytical Approach:** Shergottites and Olivine-phyric shergottites (Y980459 (Y98), NWA2626, NWA2046, NWA 1195, NWA1110, Dhofar019, SaU005, EETA79001A, DaG476), lherzolitic shergottites (LEW88516, ALH77005) and nahklites (Governador Valadares, MIL03346, Nakhla) were analyzed in this study. All of these martian meteorites have been studied to varying degrees [i.e. 4,8,9,10,11,12,13,14]. Olivine in these basalts was first imaged and mapped by SEM followed by major element analysis using a JEOL JXA-8200 electron microprobe. A suite of trace elements was analyzed (Sc, V, Cr, Ti, Mn, Co, Ni, and

Y) using a Cameca 4f ims ion microprobe and previously documented analytical approaches [13, 15]. The rationale for analyzing Y in olivine ( $D_{\text{olivine}} \sim 0.01$ ) rather than Sm ( $D_{\text{olivine}} < 0.01$ ) is that its higher abundance in olivine results in better precision. All instruments used in these analyses are housed in the Institute of Meteoritics at UNM.

### Results:

**Characteristics of olivine.** In the different martian lithologies, olivine has a wide range of morphologies and textural relationships with adjacent mineral phases. In the olivine-bearing shergottites, the large olivine “megacrysts” commonly occur in clusters and range in morphology from euhedral (i.e. Y98) to corroded/resorbed with thin Fe-rich rims (i.e. NWA1110). These textures significantly contrast with the olivine in the lherzolitic shergottites and nahklites [i.e. 12,13].

**Olivine major element chemistry.** The Mg# of early olivine in the shergottites and olivine-phyric shergottites range from 85 to 50 (Fig. 1). The olivine cores of Y98 and NWA2046 have the highest Mg#. The range observed for the shergottites overlaps with the olivine in the lherzolitic shergottites, but is significantly higher than the nahklites (45 to <25). Based on Fe-Mg exchange  $K_D$  between olivine-basalt and experimental studies [16, 17] most of the olivines are not in equilibrium with the bulk rock compositions with the exception of Y98. There are significant differences in the Mg zoning profiles between Y98 and olivine in other shergottites (i.e. Fig. 2). In all the olivines, MnO increases with decreasing Mg# from core to rim. Fig. 2 also illustrates that there can be substantial overlap in Mg# - MnO in different shergottites. This suggests that these different basalts represent similar melt compositions.

**Olivine trace element chemistry.** Ni - Co behave similarly in all martian olivines analyzed with decreasing Ni and increasing Co from core to rim (Fig. 3). The core of Y98 has the highest Ni abundance. Using core compositions of Y98 and bulk Y98 compositions appropriate D for Ni and Co for these basalts are 7.3-5.5 and 2.4-1.8, respectively. Surprisingly, most of the Ni-Co zoning trajectories for the olivine overlap except for NWA1110 and the nahklites. NWA1110 appears to be less depleted in incompatible elements than most of the other olivine-phyric shergottites [i.e. 1, 2, 3, 4] and cores have high Y. In addition to lower Ni, the olivine

in the nakhlites has higher Co. The multi-valence partitioning behavior of V in olivine reflects the early  $f_{O_2}$  crystallization conditions of basaltic magmas [17]. Vanadium in Y98 (Fig. 4), lunar basalts, and terrestrial basalts (Fig. 4B) increases with decreasing Ni from core to rim. Using the behavior of V in olivine Y98, Shearer et al. [17] estimated that the conditions of initial crystallization was at an  $f_{O_2}$  of IW+0.9. On the other hand, vanadium in olivine from all the other martian basalts decreases with decreasing Ni from core to rim indicating that the olivine in these samples is not in equilibrium with the adjacent melt.

### Discussion:

**Nature of olivine in the olivine shergottites.** There has been significant discussion concerning the origin of the olivine in the olivine-bearing shergottites (phenocrysts, megacrysts, xenocrysts). Based on such characteristics as the Mg#, V zoning, calculated  $D_{Ni,Co}$ , the olivine in Y98 are phenocrysts. Many of these same characteristics indicate that the olivines in other shergottites are not in equilibrium with the adjacent melt. However, in most cases they are not xenocrystic, but additions of olivine from the same basaltic system. This is consistent with the overlap of trace elements (Figs. 2, 3 & 4) and isotopic data [i.e. 6]. NWA1110 may be an exception [18].

**Petrogenetic relationships among the olivine-bearing shergottites.** Many of the olivine shergottites represent basalts produced by melting of reduced (IW to IW + 1) depleted mantle sources [17]. Olivine data indicates that many of the primary melts for this source had similar Ni, Co, and Mn. They exhibited more deviation in Cr and V. More evolved martian basalts such as QUE94201 were probably derived from the fractional crystallization of these basaltic melts. Other olivine-phyric shergottites (i.e. NWA1110) that appear to be derived from more enriched sources [1,2,3,5] have distinctly different olivine. These olivines are more enriched in Co, enriched in incompatible elements such as Y, and crystallized from basalt with an  $f_{O_2}$  more oxidizing than IW+1. The enrichment in Y is consistent with the composition of melt inclusions in olivine [19]. The olivine data implies that the basaltic melts represented by NWA1110 were incompatible element enriched and perhaps oxidized prior to crystallization of fairly Ni-rich olivine.

**References:** [1] Herd et al. (2002) *GCA* 66, 2025-2036. [2] Herd, C (2003) *MAPS* 38, 1993-1805. [3] Wadhwa, M. [2001] *Science*, 292, 1527-1530. [4] Goodrich et al. [2003] *MAPS* 38, 1773-1792. [5] Shih et al. (1993) *GCA* 46, 2323-2344. [6] Borg et al. (1997) *GCA* 61, 4915-4931. [7] Jones et al. (1997) *7<sup>th</sup> Goldschmidt Conf. LPI Contribution* 921, 108. [8] Barrat et al. (2002) *GCA* 66, 3505-3518. [9] Irving et al. (2002) *MAPS* 37, A69. [10] Goodrich et al. (2002) *LPSCXXXIV*, #1266. [11] Irving et al. (2004) *LPSC XXXV*, #1444. [12] McSween et al. (1979) *Science* 204, 1201-1203. [13] Treiman, A.H. (1990) *Proc. 20<sup>th</sup> LPSC*, 273-280. [14] Irving et al. (2005) *LPS XXXVI*, #1229 [15] Shearer, C.K. and Papike, J. (2005) *GCA* 69, 3445-3461. [16] McKay et al. (2004) *LPSC XXXV*, abstract # 875. [17] Shearer et al.

(2006) *Amer. Min.* 91, 1657-1664. [18] Herd, C (2006) *Amer. Min.* 91, 1616-1627. [19] Wadhwa, M. and Crozaz, G. (2002) *MAPS* 37, A145.

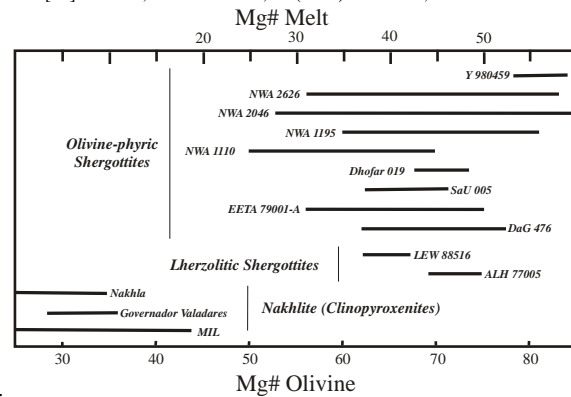


Fig. 1. Mg# of early olivine in the martian meteorites analyzed in this study. Calculated Mg# of melt in equilibrium with the olivine.

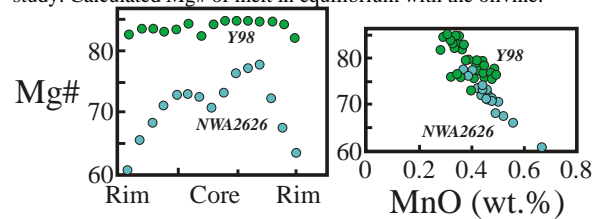


Fig. 2. Zoning profiles across two olivines in olivine-phyric shergottites illustrating differences between olivine in which calculated Mg# for melt equals bulk rock Mg# and olivine in which calculated Mg# for melt deviates significantly from bulk rock Mg#.

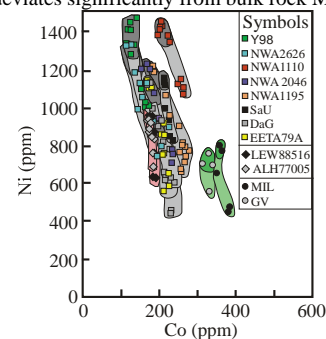


Fig. 3. Co versus Ni for olivine in shergottites (zoning shaded gray), lherzolithic shergottites (shaded orange) and nakhlites (shaded green). Core compositions for each sample are in a darker shade.

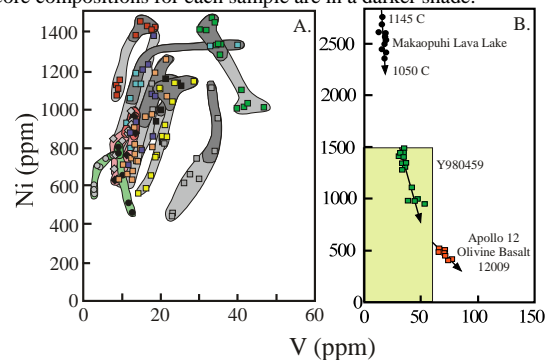


Fig. 4. A. V versus Ni for olivine in shergottites, lherzolithic shergottites and nakhlites. Symbols and shading the same as in Fig. 3. B. V versus Ni comparing olivine zoning in Y980459 (Mars), A12 olivine basalts (Moon), and basalts from the Makaopuhi lava lake (Earth).